



PERGAMON

Solid State Communications 114 (2000) 167–172

solid
state
communications

www.elsevier.com/locate/ssc

Effects of an impurity on the dissipation in a partially coherent flux-driven ring

M.T. Liu, C.S. Chu*

Department of Electrophysics, National Chiao Tung University, Hsinchu 30010, Taiwan, ROC

Received 3 December 1999; accepted 8 December 1999 by A.H. MacDonald

Abstract

We have studied a mesoscopic ring threaded by a magnetic flux that increases linearly with time. The ring is partially coherent, such that conduction electrons in the ring will encounter incoherent scatterings. In addition, the electrons encounter elastic scatterings due to the presence of an impurity in the ring. We have adopted a S -matrix model, as proposed by Büttiker [M. Büttiker, Phys. Rev. B 32 (1985) 1846; M. Büttiker, Phys. Rev. B 33 (1986) 3020], for the incoherent scatterings in this time-dependent situation. This allows us to treat the incoherent scatterings, the elastic scatterings and the coherent inelastic processes on the same footing. We have solved the problem exactly. Our results demonstrate that, in the case of a weak impurity, the lower the energies of the electrons that emanate out of incoherent scatterings, the greater will be their net contribution to the dc component I_{dc} of the induced current. In the case of a strong impurity, however, I_{dc} alternates between regions of zero and nonzero values as the chemical potential μ increases. The peak value of I_{dc} in the nonzero region increases with μ . We find that these regions of zero, and nonzero, I_{dc} correspond closely with the gaps, and the bands, respectively, of a one-dimensional energy band. All these characteristics arise from the fact that the electrons traversing the ring have their *energies* shifted gradually until their *energies* fall upon a forbidden region, where they suffer total reflection. This total reflection at the forbidden region does not occur in a ring that has a constant flux. Rather, it results from the nonadiabatic effect of the changing flux. The evolution of the nonadiabatic effects in the intermediate impurity regime has also been investigated. © 2000 Elsevier Science Ltd. All rights reserved.

Keywords: A. Nanostructures; D. Electronic band structure; D. Electronic transport

1. Introduction

A mesoscopic conducting ring threaded by a magnetic flux has been of great interest to physicists because it provides a paradigm allowing issues of fundamental importance to be tested experimentally [1]. For a fixed magnetic flux, there is an exact analogy between the single-electron states in a 1D ring and the Bloch states in a 1D crystal that has a periodic potential $V(x) = V(x + L)$, where $V(x)$ is the potential along the ring and L is the circumference of the ring [2]. The threading magnetic flux Φ plays the role of a wavevector k such that the dependence to Φ of the electronic eigen-energies in the ring can be obtained through the dispersion relation $E_n(k)$ of the corresponding 1D crystal,

where $k = -(2\pi/L)\Phi/\Phi^*$. Here $\Phi^* = hc/e$ is a flux quantum, and the band index n in $E_n(k)$ denotes the spectrum of eigen-energies for the electron states in the ring.

The concept of analogy between the single-electron states in a mesoscopic ring and that in a one-dimension crystal was extended by Büttiker et al. [2] to the case when the flux is changing linearly in time. This analogy has taken the adiabatic point of view such that the eigenstates of the ring for a fixed flux are reckoned as the momentary states of the ring with the fixed flux equaling the momentary flux.

This intuitive picture has since become the basic for the discussions of a number of physical properties proposed for mesoscopic rings. In a disordered ring, the eigen-energies over the entire range of Φ can be grouped into bands separated by energy gaps. For the case when the time rate of change in the magnetic flux is low, the induced electric field along the ring is small, and the Zener tunneling between bands can be neglected. Hence the states are caused

* Corresponding author. Tel.: +886-3-5712121, ext. 56127; fax: +886-3-5725230.

E-mail address: cschu@cc.nctu.edu.tw (C.S. Chu).

to traverse the same band periodically, with a frequency $\omega = eFL/\hbar$, so that the induced current was predicted to have no dc component but has a Josephson-like ac component [2]. Later studies show that the ring will exhibit resistive behavior, or a nonzero dc component I_{dc} , only in the presence of incoherent scatterings [3,4]. The phase randomization in the Zener tunneling amplitudes was found to lead only to the localization of the electrons in the energy space rather than leading to the resistive behavior [4]. More recently, Gorelik et al. [5] proposed the possibility of fractional pumping of energy into the ring. All these studies demonstrate beyond doubt that a driven ring is a complicated problem of which the physics depends intricately upon both the coherent and the incoherent scatterings.

Besides the adiabatic point of view, the previous studies have also assumed that major contributions to the resistive behavior arise from electrons in the vicinity of the Fermi energy. However, reasonable these two assumptions might appear to be, it is still of our interest in this paper to explore the scope of validity of these assumptions in the mesoscopic ring, where both phase coherence and topological factor together could lead to surprises. Towards this end, we propose to consider a simplest nontrivial problem that has incorporated both coherent and incoherent scatterings and yet can be solved exactly. The system is a partially coherent flux-driven ring that consists of an impurity. In solving the problem fully quantum mechanically, we have invoked an expansion scheme for the wavefunctions of the conduction electrons in the ring, and have also implemented the incoherent scattering processes in terms of an incoherent scatterer model proposed by Büttiker [6,7].

The basic wavefunctions we used for the expansion scheme is shown similar to that in a biased one-dimension system except for a phase factor that has coupled the *spatial* to the time coordinates. This phase factor effectively provides a way for the system to count the number of turns that the electron has traversed around the ring. The wavefunction of the electron is then an expansion involving many terms, each has its own time dependence and each associates with a different number of net turns traversed. The different time dependences of these terms render each term to contribute independently to I_{dc} . This is in contrast with the situation of a fixed magnetic flux in which all the terms, regardless of the number of turns traversed, have the same time dependence, and thus contribute to the current coherently.

The incoherent scatterings in the flux-driven ring have been incorporated in previous studies by introducing a relaxation time [5,8] or a cut-off time [3]. However, in the transport phenomena, the electrons that have suffered incoherent scattering should be allowed to continue their contribution to the transport current, albeit incoherently. Thus we adopt an incoherent scatterer model [7] for our time-dependent situation. This model has the incoherently

scattered electrons coupled to a reservoir through a unitary coherent scatterer [6]. The model allows us to treat the coherent and the incoherent scatterings on the same footing.

The paper is organized as follows. In Section 2 we present our formulation that incorporates the incoherent scatterings into the coherent states of the driven ring. In Section 3 we present our numerical results. Finally, in Section 4, we present a conclusion.

2. Theory

The Schrödinger equation for an electron in a ring of radius ρ , threaded by a magnetic flux Φ_B and with an impurity, is

$$\left\{ \frac{1}{2m_e^*} \left(\hbar \frac{1}{\rho} \frac{\partial}{\partial \phi} + \frac{e}{c} \frac{\Phi_B}{2\pi\rho} \right)^2 + \gamma \delta(\phi) \right\} \tilde{\Psi}(\phi, t) = i\hbar \frac{\partial}{\partial t} \tilde{\Psi}(\phi, t), \quad (1)$$

where m_e^* is the effective mass of the electron and $e > 0$.

To make this equation dimensionless, we define the length unit $R^* = \rho$, the energy unit $E^* = \hbar^2/(2m_e^*R^{*2})$, the time unit $t^* = \hbar/E^*$, the angular frequency unit $\omega^* = E^*/\hbar$, and the flux unit $\Phi^* = hc/e$. Meanwhile, the linearly increasing magnetic flux Φ_B is defined as $\omega t \Phi^*$ and $\tilde{\gamma} = E^* \gamma$. Thus the dimensionless Schrödinger equation is given by

$$\left\{ \left(-i \frac{\partial}{\partial \phi} + \omega t \right)^2 + \gamma \delta(\phi) \right\} \tilde{\Psi}(\phi, t) = i \frac{\partial}{\partial t} \tilde{\Psi}(\phi, t). \quad (2)$$

By invoking a transformation

$$\tilde{\Psi}(\phi, t) = e^{-i\omega t \phi} \Psi(\phi, t), \quad (3)$$

Eq. (2) can be cast into the form

$$\left\{ -\frac{\partial^2}{\partial \phi^2} - \omega \phi + \gamma \delta(\phi) \right\} \Psi(\phi, t) = i \frac{\partial}{\partial t} \Psi(\phi, t). \quad (4)$$

The wavefunction Ψ describes a one-dimension particle acted upon by a constant electric field. The phase factor $e^{-i\omega t \phi}$ in Eq. (3) is suggestive that an electron will gain, or lose, an *energy* of $2\pi\omega$ if it moves, respectively, around the ring once counter-clockwisely or clockwisely. This is consistent with the direction of the induced electric field along the ring. This phase factor plays a very important role in imposing the single-valueness in $\tilde{\Psi}$ at all time, and at $\phi = 0$, and 2π . To facilitate the matching, we define in the following a basic set of wavefunctions for the driven ring. The actual wavefunction $\tilde{\Psi}$ for the driven ring that satisfies the single-valueness is constructed out of this basic set of wavefunctions. The basic wavefunctions representing counter-clockwise-moving particles are given by

$$\tilde{\Psi}^{(+)}(\phi, t; \epsilon) = \frac{\sqrt{\zeta(\phi, \epsilon)} H_{1/3}^{(1)}[2/3 \zeta^{3/2}(\phi, \epsilon)]}{(6\sqrt{\omega/\pi})^{1/2}} e^{-i(\epsilon + \omega \phi)t}, \quad (5)$$

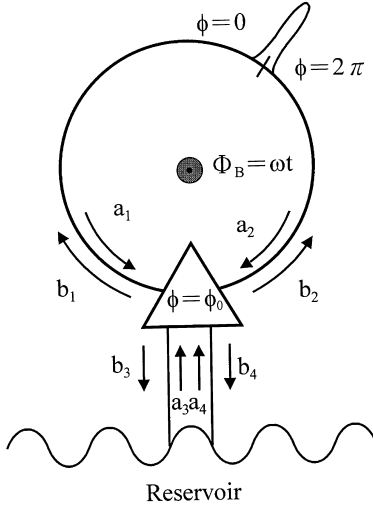


Fig. 1. A partially coherent flux-driven ring. The flux, represented by the center shaded circle and directed out of the page, is linear in time with $\Phi_B = \omega t$. The ring is coupled via a coupler, depicted by the triangle, to a reservoir, depicted by the wavy line. The electron coordinate ϕ increases in the counter-clockwise direction along the ring. The impurity is at $\phi = 0$.

whereas the basic wavefunctions representing clockwise-moving particles are given by

$$\tilde{\Psi}^{(-)}(\phi, t; \epsilon) = \frac{\sqrt{\zeta(\phi, \epsilon)} H_{1/3}^{(2)}[2/3 \zeta^{3/2}(\phi, \epsilon)]}{(6\sqrt[3]{\omega/\pi})^{1/2}} e^{-i(\epsilon + \omega\phi)t}. \quad (6)$$

Here $\zeta(\phi, \epsilon) = \omega^{1/3}(\phi + \epsilon/\omega)$, and $H_{1/3}^{(1)}(z)$, $H_{1/3}^{(2)}(z)$ are Henkel functions. The energy parameter ϵ is a continuous variable.

These basic wavefunctions are normalized with unit particle current, in the unit of $-eE^*/\hbar$. This choice of the normalization for the basic wavefunctions is deemed necessary, as pointed out by Stone and Szafer [9], when invoking the incoherent scatterer model of Büttiker [6] for the incoherent processes in our system.

The incoherent scatterer model consists of a coupler that couples the electrons in the system to a reservoir. Current that flows out of the ring, and into the reservoir, will be reinjected back into the system according to the distribution in the reservoir. There is no phase correlation between the currents that flow in and flow out of the reservoir. It is through this process that phase coherence in the particles is lost. Further, by describing the coupler in terms of an energy-independent \mathbf{S} , the incoherent processes are cast into a scattering problem. The \mathbf{S} matrix [6], given by

$$\mathbf{S} = \begin{bmatrix} 0 & \sqrt{1-\alpha} & \sqrt{\alpha} & 0 \\ \sqrt{1-\alpha} & 0 & 0 & \sqrt{\alpha} \\ \sqrt{\alpha} & 0 & 0 & -\sqrt{1-\alpha} \\ 0 & \sqrt{\alpha} & -\sqrt{1-\alpha} & 0 \end{bmatrix}, \quad (7)$$

couples incoming waves, with current amplitudes $\mathbf{a} = (a_1, a_2, a_3, a_4)$, to the outgoing waves, with current amplitudes $\mathbf{b} = (b_1, b_2, b_3, b_4)$, through the relation $\mathbf{b}^T = \mathbf{S}\mathbf{a}^T$. The notation convention for these amplitudes is shown in Fig. 1.

The form of \mathbf{S} is chosen such that it is unitary as long as the basic wavefunctions are all normalized to a unit current. The coupling parameter α , with $0 \leq \alpha \leq 1$, denotes the extent that the ring couples with the reservoir. In the limiting case of $\alpha = 1$, the particle will entirely lose track of its phase every time it encounters the incoherent scatterer. In the other limiting case, when $\alpha = 0$, the ring and the reservoir are decoupled. For definiteness, we choose the coupler to locate at $\phi = \phi_0$. Our results, however, turn out to be independent of ϕ_0 . This reassures us, in part, the credibility of the \mathbf{S} -matrix incoherent scatterer model for this time-dependent problem.

The basic wavefunctions in leads $i = 3, 4$ are

$$Y^{(+)}(x_i, t; \epsilon) = \frac{e^{-i(\epsilon t - \sqrt{\epsilon} x_i)}}{(2\sqrt{\epsilon})^{1/2}} \quad (8)$$

for particles incident upon the coupler, and

$$Y^{(-)}(x_i, t; \epsilon) = \frac{e^{-i(\epsilon t + \sqrt{\epsilon} x_i)}}{(2\sqrt{\epsilon})^{1/2}} \quad (9)$$

for particles leaving the coupler. The coordinates $x_i = 0$ at the coupler.

In the following, we first consider electrons incident upon the ring within an energy interval $d\epsilon$ from the reservoir via either leads 3 or 4. The incident current is $\mathcal{N}(\epsilon) = 2f(\epsilon) d\epsilon$, where $f(\epsilon)$ is the Fermi–Dirac distribution for the reservoir with a chemical potential μ , and the spin degeneracy has been included. The incident current amplitude is then chosen to be $\sqrt{\mathcal{N}(\epsilon)}$.

For electrons incident from the lead $i = 4$, the wavefunctions in the leads 4 and 3 are, respectively, given by

$$\tilde{\Psi}_4 = \sqrt{\mathcal{N}(\epsilon)} Y^{(+)}(x_4, t; \epsilon) + \sum_n r_{44}(n) Y^{(-)}(x_4, t; \epsilon_n), \quad (10)$$

and

$$\tilde{\Psi}_3 = \sum_n t_{34}(n) Y^{(-)}(x_3, t; \epsilon_n). \quad (11)$$

The coefficients $t_{34}(n)$, and $r_{44}(n)$ are the reflection current amplitudes in leads 3 and 4, respectively. The index n denotes the possible reflected electron energies that result from the action of the time-varying flux in the ring. The wavefunctions in the ring within the region $0 < \phi < \phi_0$ is written as

$$\tilde{\Psi}_1 = \sum_n [A_n(\epsilon_n) \tilde{\Psi}^{(+)}(\phi, t; \epsilon_n - \omega\phi_0) + B_n(\epsilon_n) \tilde{\Psi}^{(-)}(\phi, t; \epsilon_n - \omega\phi_0)], \quad (12)$$

and, within the region $\phi_0 < \phi < 2\pi$, is written as

$$\tilde{\Psi}_{\text{II}} = \sum_n [C_n(\epsilon_n) \tilde{\Psi}^{(+)}(\phi, t; \epsilon_n - \omega\phi_0) + D_n(\epsilon_n) \tilde{\Psi}^{(-)}(\phi, t; \epsilon_n - \omega\phi_0)], \quad (13)$$

where $\epsilon_n = \epsilon + 2\pi\omega n$. These wavefunctions, including their energy arguments $\epsilon_n - \omega\phi_0$, are written in the form that facilitates the matching of the wavefunctions at $\phi = \phi_0$, and at all times. Without loss of generality, we let the impurity to locate at $\phi = 0$, with a potential $\gamma\delta(\phi)$. The matching of the wavefunctions at $\phi = 0$ and 2π and at all times gives us the relations

$$\begin{pmatrix} A_n \\ D_{n-1} \end{pmatrix} = \mathbf{S}_c(\epsilon_n - \omega\phi_0) \begin{pmatrix} B_n \\ C_{n-1} \end{pmatrix}, \quad (14)$$

where

$$\mathbf{S}_c(\epsilon_n - \omega\phi_0) = \frac{1}{1 + i\gamma|Z|^2} \begin{pmatrix} -i\gamma Z^2 & 1 \\ 1 & -i\gamma Z^{*2} \end{pmatrix}, \quad (15)$$

and

$$Z = \frac{\sqrt{\chi_n} H_{1/3}^{(2)}[2/3\chi_n^{3/2}]}{(6\sqrt[3]{\omega/\pi})^{1/2}}. \quad (16)$$

Here $\chi_n = \chi(\epsilon_n - \omega\phi_0) = \omega^{1/3}(\epsilon_n/\omega - \phi_0)$.

The relations between the coefficients A_n, B_n, C_{n-1} and D_{n-1} , given by Eq. (14), and the connections of these coefficients to that in leads 3 and 4, obtained via the \mathbf{S} matrix in Eq. (7), can be used to solve the coefficients simultaneously. However, a direct approach to solving these simultaneous equations is very inefficient. An alternative approach that we have undertaken is to solve, separately, for the reflected wave of a counter-clockwise-moving injected wave, and that of a clockwise-moving injected wave. The multiple scatterings in these two separate calculations can be treated exactly and efficiently, using the transfer matrix method. The total wavefunction is then obtained by coupling the results from the above two separate calculations via the \mathbf{S} matrix to the incident amplitude.

We note that in the case of the counter-clockwise-moving injected wave, the energy of the electron increases by $2\pi\omega$ for every additional counter-clockwise loop it traversed. This looping cannot keep on indefinitely because of the incoherent processes and the impurity scattering. Hence, our actual calculation involves choosing a sufficiently large number N_{max} for the maximum counter-clockwise loopings traversed by the electron. We then calculate the reflected wave, and the coefficients for each looping by invoking the transfer matrix method. A reasonable choice of N_{max} has to produce the converged values of the reflection coefficients.

The above method can be applied, essentially, to the case of the clockwise-moving injected wave, except now that the energy of the electron decreases by $2\pi\omega$ for every

additional clockwise loop it traversed. This lowering of energy continues until, at the N th clockwise loop, the electron encounters its forbidden region, where the wavefunction becomes evanescent, and the electron will suffer total reflection. Here $N = [\epsilon/(2\pi\omega)]$ and $[x]$ denotes the largest integer smaller than or equal to x . Subsequently, the relation between the coefficients in this last looping is given by either $A_{-N}/B_{-N} = e^{i\pi/3}$, or $C_{-N}/D_{-N} = e^{i\pi/3}$, depending on the location of this so-called classical turning point.

It could happen that, in the presence of incoherent processes, the electron may not even be able to reach its classical turning point. This is the case when $N > N'_{\text{max}}$, where N'_{max} , like N_{max} in the counter-clockwise loop, is the maximum number of clockwise loop in which the traversing electron can maintain its coherence.

For the electrons incident from the lead $i = 3$, the wavefunctions in the leads 3 and 4 are, respectively

$$\tilde{\Psi}_3 = \sqrt{\mathcal{N}'(\epsilon)} Y^{(+)}(x_3, t; \epsilon) + \sum_n r_{33}(n) Y^{(-)}(x_3, t; \epsilon_n) \quad (17)$$

and

$$\tilde{\Psi}_4 = \sum_n t_{43}(n) Y^{(-)}(x_4, t; \epsilon_n). \quad (18)$$

The coefficients $r_{33}(n)$, and $t_{43}(n)$ are the reflection current amplitudes in leads 3 and 4, respectively. Further, the wavefunctions in the ring are in a form similar to those in Eqs. (12) and (13), except that the coefficients A_n, B_n, C_n , and D_n are replaced by $\tilde{A}_n, \tilde{B}_n, \tilde{C}_n$, and \tilde{D}_n . Again, following the same aforementioned matching procedure, we obtain all these coefficients.

Finally, the total dc particle current I_{dc} , averaged over a time period of $1/\omega$, and at zero temperature, can be expressed in terms of the above wavefunction expansion coefficients, given by

$$I_{\text{dc}} = 2 \int_0^\mu \left\{ \sum_{n=0}^{-N} (|A_n|^2 - |B_n|^2) + \sum_{n=0}^{N_{\text{max}}} (|C_n|^2 - |D_n|^2) + \sum_{n=0}^{-N} (|\tilde{A}_n|^2 - |\tilde{B}_n|^2) + \sum_{n=0}^{N_{\text{max}}} (|\tilde{C}_n|^2 - |\tilde{D}_n|^2) \right\} d\epsilon, \quad (19)$$

where μ is the chemical potential.

We have checked the convergence of our results with respect to our choice of N_{max} , and have also checked that the net dc current I'_{dc} between the ring and the reservoir is zero.

3. Results

In this section, we present the effects of impurities on the dissipation in a partially coherent ring by plotting I_{dc} versus μ for a number of impurity strengths. The physical parameters we choose are consistent with that of

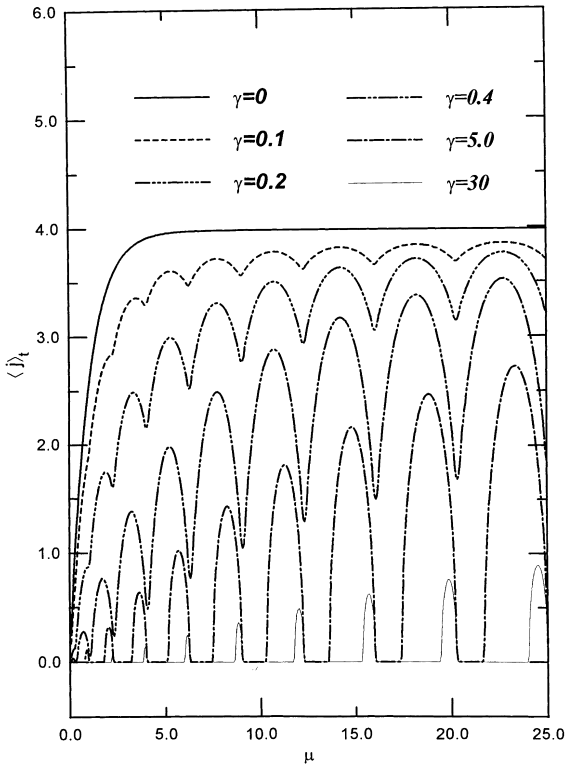


Fig. 2. Total dc component I_{dc} as a function of μ for $2\pi\omega = 0.01$, $\alpha = 0.01$ and for $\gamma = 0.0, 0.1, 0.2, 0.4, 5.0$, and 30 .

a semiconductor ring, with $R^* = 150$ nm and $m_e^* = 0.067m_e$. Since our emphasis is upon the interplay between the coherent and the dissipative nature in the mesoscopic ring, we present only the cases for the small α regime. Hence in Fig. 2, we choose $\alpha = 0.01$. In addition, we choose $2\pi\omega = 0.01$, which corresponds to an induced electromotive force $2\pi R^* F = 2.5 \times 10^{-7}$ V in the ring. Finally, the curves for the six impurity strengths ($\gamma = 0.0, 0.1, 0.2, 0.4, 5.0$, and 30) in Fig. 2 present the entire spectrum of the impurity effects: from the weak impurity regime all the way to the strong impurity regime.

The general features presented in Fig. 2 are summarized in the following paragraphs. For a smooth ring, when $\gamma = 0$, I_{dc} is shown to increase with μ initially and saturates in the larger μ regions. This solid curve in Fig. 2 also serves as an upper bound to that for rings with impurities, because I_{dc} is lowered in the presence of an impurity. When the impurity is weak, such as represented by the dashed curve ($\gamma = 0.1$) in Fig. 2, the overall trend in $I_{dc}(\mu)$ follows that of the smooth ring, except that I_{dc} shows additional oscillatory behavior.

The amplitudes of this oscillation increase with the strength of the impurity as indicated by the curves for $\gamma = 0.2$ and 0.4 , while the oscillation pattern evolves into finger-like structures separated by dips. The values of I_{dc} at both the maxima of these finger-like structures and the minima of

these dips increase monotonically with μ and saturate towards the large μ region. In addition, these I_{dc} values decrease with increasing γ . Therefore, further increase in the strength of the impurity, as indicated by the curves for $\gamma = 5.0$ and 30 , causes the dips to drop eventually to zero. By then the dissipation enters its strong impurity regime where the dips are flattened into $I_{dc} = 0$ plateaus. In the following paragraphs, we will present a physical picture explaining the characteristics in all these dissipation regimes.

Before we proceed further, we recall, from Eq. (19), that I_{dc} is an energy integral that includes contribution from all energies below μ . These energies are the energies of the electrons that are emanating out of incoherent scatterings. These electrons are equally likely to be reinjected into the ring as clockwise-moving or counter-clockwise-moving states, because of the symmetry in the incoherent scatterings. However, the subsequent propagation of the electrons may or may not preserve this symmetry. We will address this issue of symmetry for the subsequent propagation later. But if there were to be perfect symmetry between the subsequent propagation for the clockwise and the counter-clockwise injected electrons, the contribution to I_{dc} from these emanating electrons would exactly cancel each other. Hence, it is understandable that, for a given emanating energy interval $d\epsilon$, the more asymmetric it is in the subsequent propagation, the greater will be the net contribution to I_{dc} .

In the case of a smooth ring, the current I_{dc} increases initially with μ but saturates in large μ regions. This demonstrates that the greater the energies of the electrons that emanate out of incoherent scatterings, the smaller will be their net contribution to I_{dc} . Particularly, in the saturation region, the electrons emanate with energies near μ do not contribute to I_{dc} , while the saturated I_{dc} value is contributed from electrons that emanate with much lower energies. These features can be understood from considering the symmetry in the propagation directions.

One might expect, in the case of a time-varying magnetic flux, that the induced electric field in the ring should forbid any possibilities of symmetry between the clockwise and counter-clockwise propagation. This is certainly so for the case of large induced electric field. But if the induced electric field is low enough ($2\pi\omega \ll \mu$), as it is the case in Fig. 2, where $2\pi\omega = 0.01$, the symmetry between the two propagation directions within a few loopings still holds, except for a phase factor $e^{-i\omega t/\phi}$. This phase factor, as has been discussed in the previous section, causes the energy of the electron to increase or decrease by $2\pi\omega$ for every loop it traversed. Taking ω as positive, the energy of the electron will increase, or decrease, for every counter-clockwise, or clockwise, loop it traversed, respectively. This small shift in energy does not affect the symmetry if only a few loopings were to traverse. However, if there were no restriction on the number of coherent loopings the electron can traverse, the effect of the energy shift, accumulated in due loopings, would violate the symmetry significantly. It then occurs

that the clockwise-moving electrons will encounter their classical turning point and suffer total reflection. Since the number of loopings the electrons traverse before they encounter their classical turning point is $N = [\epsilon/2\pi\omega]$, the symmetry can be restored if a maximum number N_{\max} ($N_{\max} \ll N$) of coherent loopings can be imposed upon the electrons.

Here, the incoherent scatterings provide us a natural restriction upon the number of net loopings, with $N_{\max} \approx 1/\alpha$. Therefore, for a given α and ω , the contribution from emanating electrons, with energy ϵ , falls into two regimes. In the small ϵ regime, where $N < N_{\max}$, the electrons can reach their forbidden region coherently, hence violating the symmetry, and contribute significantly to I_{dc} . This regime is characterized by a rapid change in I_{dc} . The other is the large ϵ regime, where $N \gg N_{\max}$, such that the electrons cannot reach their forbidden region, hence restoring the symmetry, and having resulted in zero contribution to I_{dc} . This regime is characterized by a saturated I_{dc} . The physical picture presented above is supported by an analytic solution for a partially coherent flux-driven smooth ring [10].

The above physical picture can be extended to the case of the strong impurity regime, such as the $\gamma = 5.0$ curve in Fig. 2. This curve exhibits regions of zero I_{dc} in between finger-like structures. The finger-like structures are symmetric in μ and consist of a sharp rise in I_{dc} followed by a sharp drop in I_{dc} . When we look into the energy band structure of a one-dimensional crystal formed by the $\gamma = 5.0$ impurities, and separated by a period of L , we find that the energy gaps overlap exactly with the regions of zero I_{dc} . This shows, first of all, that the impurities have brought forth, to the electrons in the ring, multiple gap regions, or, according to our previous discussions, multiple forbidden regions. Secondly, the exact overlapping shows that band-edge is well defined, which in turn shows that Zener tunneling between energy bands is insignificant. Therefore, electrons with emanating energies that fall within an energy gap do not contribute to I_{dc} .

However, for the finger-like structures, where the emanating energies fall within an energy band, there are two forbidden regions, of which the turning points occur at the upper and the lower band edge. The clockwise-moving injected electrons will encounter their forbidden region at the lower band edge while the counter-clockwise-moving injected electrons will encounter their forbidden region at the upper band edge. Therefore, contribution from emanating energy ϵ , close to the lower band edge will be dominated by counter-clockwise-moving electrons while that from ϵ , close to the upper band edge will be dominated by clockwise-moving electrons. The sharp rise and drop of I_{dc} in a finger-like structure then results from the breaking of

the propagation symmetry. The multiple finger-like structures demonstrate that the presence of impurities in the ring gives rise to multiple turning points, thus causing the rapid change in I_{dc} to occur in many different μ regions.

Finally, the intermediate impurity regime, as shown by the $\gamma = 0.2$, and 0.4 curves in Fig. 2, exhibits a reasonable and continuous transition connecting the weak and the strong impurity regimes. It is believed that Zener tunneling comes into play in this regime.

4. Conclusion

We have solved exactly the dissipation characteristics of a partially coherent flux-driven ring in the presence of an impurity. A physical picture is proposed to explain the general dissipative features. In particular, our results demonstrate the close relation between the breaking of the propagation symmetry and the rapid change of I_{dc} in the ring. It was predicted by Büttiker et al. [2], using the adiabatic point of view, that $I_{dc} = 0$ whenever Zener tunneling is negligible. This prediction is consistent with the zero I_{dc} regions in our results, but not with the finger-like structures in the $I_{dc}(\mu)$ curve. Thus, the finger-like structures found in this work are the nonadiabatic results. The interesting possible manifestation of this nonadiabatic feature in the case of an oscillatory magnetic flux, and in the case when electron–electron interactions are taken into account, is left to future investigations.

Acknowledgements

This work was supported in part by the National Science Council of the Republic of China through Contract No. NSC89-2112-M-009-019.

References

- [1] Y. Imry, Introduction to Mesoscopic Physics, Oxford University Press, New York, 1997.
- [2] M. Büttiker, Y. Imry, R. Landauer, Phys. Lett. A 96 (1983) 365.
- [3] Y. Gefen, D. Thouless, Phys. Rev. Lett. 59 (1987) 1752.
- [4] G. Blatter, D.A. Browne, Phys. Rev. B 37 (1988) 3856.
- [5] L. Gorelik, S. Kulinich, Yu. Galperin, R.I. Shekhter, M. Jonson, Phys. Rev. Lett. 78 (1997) 2196.
- [6] M. Büttiker, Phys. Rev. B 32 (1985) 1846.
- [7] M. Büttiker, Phys. Rev. B 33 (1986) 3020.
- [8] R. Landauer, M. Büttiker, Phys. Rev. Lett. 54 (1985) 2049.
- [9] A.D. Stone, A. Szafer, IBM J. Res. Develop. 32 (1988) 384.
- [10] M.T. Liu, C.S. Chu, unpublished.